J Mater Sci (2010) 45:2916–2920
DOI 10.1007/s10853-010-4283-0

Microwave synthesis and physical characterization of tin(II) phosphate glasses

Nicolas Hémono · Sébastien Chenu · Ronan Lebullenger · Jean Rocherullé · Vincent Kéryvin · Alain Wattiaux

Received: 1 October 2009 / Accepted: 28 January 2010 / Published online: 13 February 2010

Abstract Tin phosphate glasses in the $SnO–P_2O_5$ binary diagram have been prepared by using a domestic microwave-heating device. Microwaves provide an extremely facile and automatically temperature-controlled route to the synthesis of glasses due to the specific dielectric properties of each chemical composition. Typical melting time is no longer than 10 min, limiting the oxidation of Sn^{2+} and the melt can be quenched into glass. The glass transition temperature increases with the SnO content confirming the depolymerization of the vitreous network, as expected by the relative fraction of the different Q^n structural units deduced from NMR experiments. Concerning the mechanical properties, the Vickers hardness and the fracture toughness decrease while the thermal expansion coefficient and the different elastic moduli remain constants. These results confirm that those characteristics are not very sensible to structural considerations. On the contrary, the chemical durability of $Sn_2P_2O_7$, determined from the weight loss method, is 300 times higher than that of $Sn(PO_3)_2$. Furthermore, $Sn_2P_2O_7$ is the only glass composition that exhibits a devitrification phenomenon leading to the low-temperature phase of the crystalline tin(II) pyrophosphate.

N. Hémono · S. Chenu · R. Lebullenger · J. Rocherullé (✉)
UMR CNRS 6226 Equipe Verres et Céramiques, Université de Rennes I, 35042 Rennes, France
e-mail: Jean.rocherulle@univ-rennes1.fr

V. Kéryvin
LARMAUR FRE CNRS 2717, Université de Rennes I, 35042 Rennes, France

A. Wattiaux
UPR CNRS 9048, ICMCB 86, 33608 Pessac, France

Introduction

Sealing glasses are used to join glasses, metals, ceramics and composites. They are formulated to seal at suitable temperature and to present coefficient of thermal expansion (CTE) to match several materials. Donald [1] has listed a large number of possible compositions.

Pb-based sealing glasses, such as $PbO–B_2O_3–SiO_2$ or $PbO–ZnO–B_2O_3$ are employed for commercial sealing [2]. However, lead oxide is associated with deleterious health and environmental effects [3]. For this reason, many searches have been conducted for glass compositions with low glass transition temperature (T_g) as possible alternatives to Pb-based sealing glasses. Phosphate glasses are characterized by lower glass transition temperatures and higher coefficients of thermal expansion than borate and silicate glasses. Furthermore, tin oxide is considered as alternative to lead oxide due to its similar properties [4]. In this article, tin phosphate glasses in the $SnO–P_2O_5$ binary composition diagram have been examined as base materials for potential replacement of lead containing glasses in sealing applications. In a general way, the synthesis of tin phosphate glasses by heating up to 1,000 °C by means of an electric furnace conducts to the crystallization of SnP_2O_7 (ICDD PDF file No 45-0035). The occurring of this crystalline phase is due to the oxidation of Sn^{2+} into Sn^{4+} as mentioned in previous results [5]. To avoid the crystallization of SnP_2O_7, a microwave oven has been used for glass synthesis. Microwave heating is based on electromagnetic induction of heat within the glass bulk. In glass science, it has been reported that various glass compositions could be prepared in such a way [6–8]. In this way, the heating rate of the material is fast, the melting temperature is lower than 1,000 °C and the refining time is drastically reduced due

to the homogeneous heating of the sample compared to conventional heating.

The glass forming range has been determined in the binary composition diagram. The thermal and mechanical properties, the chemical durability of glass compositions, for which the tin oxide molar content is greater than 50%, have been discussed in terms of the Q^n structural units determined from ^{31}P MAS NMR experiments.

Experimental

Glasses have been prepared from batches of reagent grade SnO and $NH_4H_2PO_4$. The batches were heated in pure silica crucibles, stood on a fired brick in the oven, during 10 min by using microwave irradiation. Then, the melts have been quenched in air by pouring in a brass mould and annealed for 30 min at the glass transition temperature. The microwave-heating device is a domestic oven (2.45 GHz) with a nominal power of 750 W. An optical pyrometer (IGA 140 Impac) has been used to monitor the temperature of the melt through a hole drilled on the top of the cavity.

The limits of the glass forming region were checked by X-ray powder diffraction. Data were collected with a PHILIPS diffractometer using Cu$K\alpha$ radiation ($\lambda K\alpha_1 = 1.5406$ Å, $\lambda K\alpha_2 = 1.5444$ Å) selected with a diffracted-beam graphite monochromator and the Bragg Brentano optics. The ICDD PDF2 database, available in the program search/match from the PC software package X'PERT supplied by PHILIPS, was used in order to reveal possible crystallization.

The Mössbauer spectra were obtained using a constant acceleration spectrometer with a room temperature $CaSnO_3$ source (119Sn) in transmission geometry. The samples contained 15 mg of natural tin/cm^2. For such a concentration, line broadening due to thickness effects can be neglected. The spectra at 4.2 and 293 K were recorded using a variable temperature cryostat. The spectra were fitted as a sum of Lorentzians by least square refinements.

The solid state NMR experiments were performed at 293 K with a BRUKER "AVANCE 300" spectrometer operating at 7 Tesla for the static magnetic field B_0. The ^{31}P MAS NMR spectra were obtained with a resonance frequency of 121.53 MHz, a recycle delay equal to 5 s and a $\pi/2$ pulse length equal to 2 μs. A total of 256 scans were accumulated for every spectrum. The ^{119}Sn spectra were performed at a resonance frequency of 119.92 MHz and a Hahn-Echo pulse sequence was used with a $\pi/2$ pulse equal to 2 μs. The recycle delay was 10 s and 30,000 scans were necessary to obtain an acceptable signal-to-noise ratio. The deconvolution of the spectra was carried out by means of the DMFIT software [9].

Differential thermal analysis (DTA) experiments were performed with a TA Instruments Model SDT 2960. DTA scans were recorded at 10 °C/min. The overall accuracy of this instrument is expected to be within ±1 K. The coefficients of thermal expansion (CTE) were measured by a TA Instruments Model TMA 2940, with a 2 °C/min heating rate and a preload force of 0.1 N. The precision of the CTE determination is $\pm 2 \times 10^{-7}$ K^{-1}.

The density of glasses was measured by the Archimedes method using ethanol as the suspending medium. The error in the determination of the density is ±0.02 g cm^{-3}.

Young's modulus (E), bulk modulus (G) and shear modulus (K) were measured by the ultrasonic velocity technique. This technique is based on time-of-flight measurements using the pulse-echo technique [10] with ±2 GPa as the accuracy value. Vickers microhardness (H_v) and the indentation fracture toughness (K_{1c}) were measured by the indentation technique using a 50 g load applied for 5 s with a Matsuzawa Digital Microhardness Tester MXT 70 with an accuracy of 2.5%. The chemical durability was evaluated from the weight loss of bulk samples immersed in water at 95 °C during 7 days. A constant ratio sample surface/solution volume of 0.1 cm^{-1} was maintained in order to compare the results. The faces of the samples were polished with 1,200 grit SiC paper and cleaned in acetone. After each corrosion test, the samples were dried at 100 °C until the weight remained constant. The dissolution rate (DR) of samples was calculated from the measured weight loss (ΔW), sample surface area (SA) and time of immersion (t), using the following equation:

$$\mathrm{DR} = \frac{\Delta W(\mathrm{mg})}{\mathrm{SA}(\mathrm{cm}^2) \times t(\mathrm{day})}.$$

The precision is expected to be better than 5%.

Results and discussion

Figure 1 shows the temperature of the melt for two compositions as a function of the heating time. In all cases, the weight of the batch and the position of the crucible were remained unchanged. At first, there is a fast and linear temperature raise then it reaches a constant value, which depends on the batch composition. The glass forming range, given in Fig. 2, has been determined at temperatures up to 950 °C with a melting time, which does not exceed 10 min. It was possible to obtain pure glasses for a tin oxide content up to 72 mol.%. The absence of any crystalline phase, after melting and quenching, has been checked by X-ray powder diffraction analysis. Usually, the melting in air at temperatures up to 1,000 °C oxidizes Sn^{2+} in Sn^{4+} providing the crystallization of SnP_2O_7. Furthermore, Mössbauer spectroscopy has been used to determine the Sn^{4+}/Sn_{total}

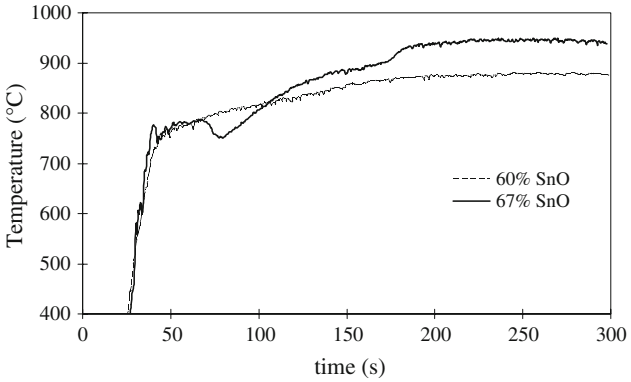

Fig. 1 Melting temperature profile as a function of heating time for glasses with different chemical compositions

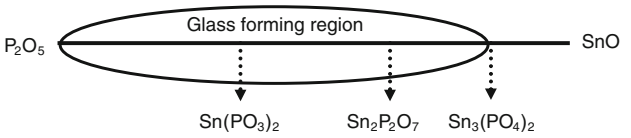

Fig. 2 Glass forming region in the SnO–P_2O_5 compositional binary diagram

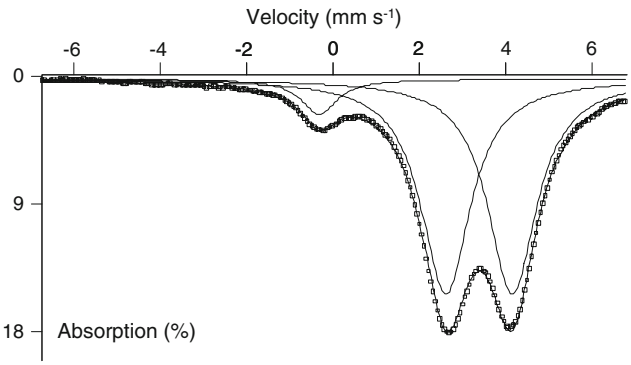

Fig. 3 Mössbauer spectrum for the $Sn_2P_2O_7$ glass composition ($T = 4.2$ K)

ratio in the case of the pyrophosphate glass composition for which the melting temperature was the highest one. The Mössbauer spectrum recorded at 4.2 K, displayed in Fig. 3, can be decomposed into three peaks: a quadrupolar symmetric doublet characteristic of Sn(II), and a singlet corresponding to Sn(IV). The quadrupolar splitting of Sn(IV) is very small, so it appears as a singlet. The Sn(IV) signal is weak, in accordance with a low concentration in the glass. Thus, the asymmetry of the Sn(II) doublet, for the spectrum recorded at 293 K, is not due to overlapping with a Sn(IV) line. The asymmetry of the Sn(II) doublet arises from an anisotropy of the Debye–Waller factor (Goldanskii–Karyagin effect). The Mössbauer spectrum recorded at 4.2 K being symmetric, it confirms the Goldanskii effect, due to the vibrational anisotropy associated with the presence of the 5 s^2 lone pair of Sn(II). In addition, another experiment performed in the same conditions in presence of a reducing agent (i.e. graphite) yields to the same result. In all cases, the Sn^{4+} content (determined from subspectral areas) is lower than 6 at.%.

The addition of tin oxide in the phosphorous matrix leads to a depolymerization of the network. Each SnO replaces two P–O–P links by two P–O–Sn links according to the following equation [11, 12]:

$$2Q^n + SnO \rightarrow 2Q^{n-1}.$$

Q^2-type sites are present in the metaphosphate glass (O/P = 3) and Q^1-type sites in the pyrophosphate glass (O/P = 3.5). Between these two compositions, the vitreous network is composed of the two types. The decomposition of the ^{31}P MAS NMR spectra gives the proportions of Q^n-type sites (see Fig. 4). As evidence, Q^1-type tetrahedra (i.e. $(P_2O_7)^{4-}$ diphosphate unit) are created to the detriment of the Q^2-type tetrahedra (i.e. (PO_3^-) metaphosphate unit).

^{119}Sn NMR spectra are shown in Fig. 5. The broad spectra are characteristic of Sn(II). Indeed, the large electronic shielding of the Sn(II) induces a large chemical shift

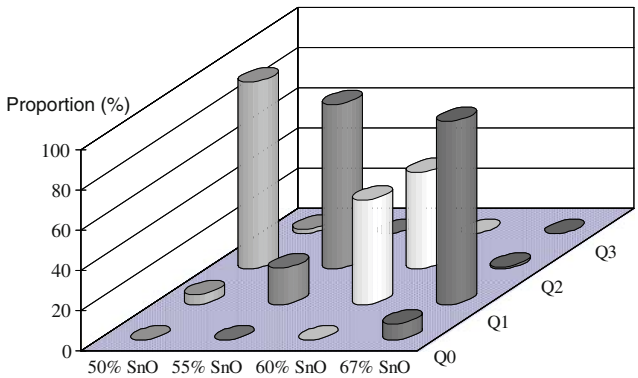

Fig. 4 Distribution of the Q^n-type sites as a function of the tin oxide molar content

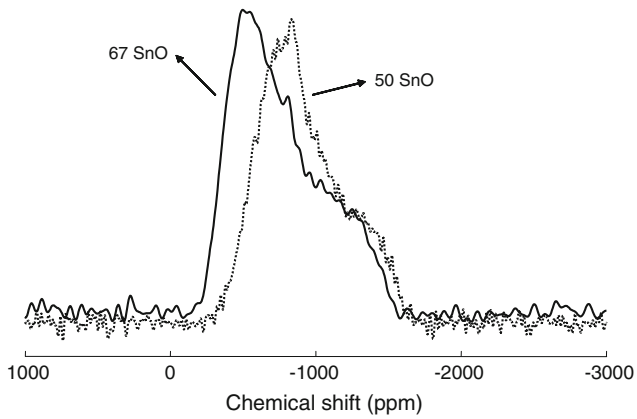

Fig. 5 ^{119}Sn NMR spectra (static) of $xSnO - (100 - x)P_2O_5$ ($x = 50, 67$)

anisotropy that cannot be suppressed by magic angle spinning. The ^{119}Sn spectra of xSnO – (100 − x)P_2O_5 (x = 50, 67) glasses show a shift of Sn(II) resonance towards the positive values, also reported in [5], when x increases from 50 to 67. In other words, the nucleus becomes less shielded. The possible causes of this are change in next nearest neighbour (Sn for P substitution), change in coordination number, change in hybridization and extent of the lone pair in space. Nevertheless, the electronegativity of P is not much greater than that of Sn and as a consequence, the next nearest neighbour atoms have only little direct effect on the shielding of the nucleus. In such phosphate glasses, the coordination number of tin is expected to be constant and equals to three [5], thus the deshielding is likely dominated by the lone pair of electrons, which can extent in space when the number of nearest neighbour oxygens is greater.

The evolutions of the density and of the glass transition temperature are shown in Fig. 6. T_g values are increasing with addition of tin oxide. This is a consequence of the depolymerization of the vitreous network. Nevertheless, this evolution is not so important when compared to systems such as PbO–P_2O_5 or ZnO–P_2O_5 [13]. In the same way, the glass density is increasing with addition of SnO. It can simply be explained by the tin for phosphorous substitution in terms of the elementary atomic weight. Contrary to T_g and density, the CTE values remain constant and close to 140 × 10^{-7} K^{-1}.

The variations of the elastic moduli are shown in Fig. 7. The Young's modulus (E), bulk modulus (G) and shear modulus (K) are fairly constant. These values are lower than those of silicates glasses. Thus, the network-depolymerization effect has no consequence on elastic moduli values. On the other hand, Vickers microhardness (H_v) and fracture toughness (K_{1c}) are clearly linked to the % Q^1-type sites (see Fig. 8). The microhardness is relatively constant for a Q^1 proportion less than 50% and then decreases drastically when this proportion becomes greater than 50%. On the contrary, the fracture toughness

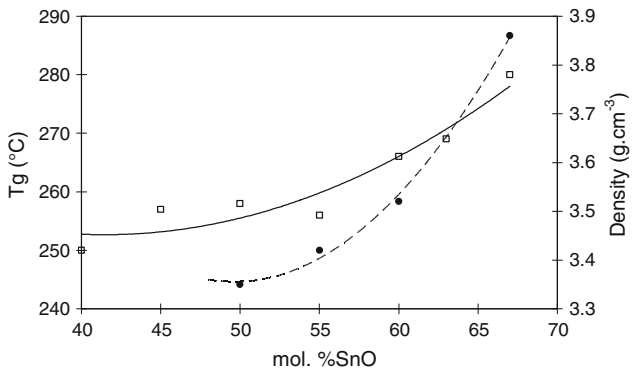

Fig. 6 Variations of the glass transition temperature (*solid line*) and the density (*dotted line*) as a function of the tin oxide molar content

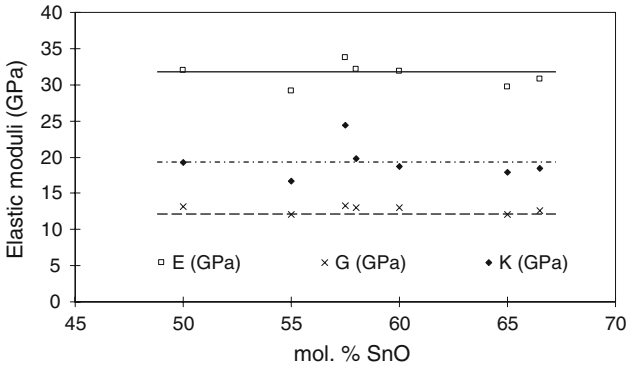

Fig. 7 Variations of the elastic moduli as a function of the tin oxide molar content. The lines are only guides for eyes

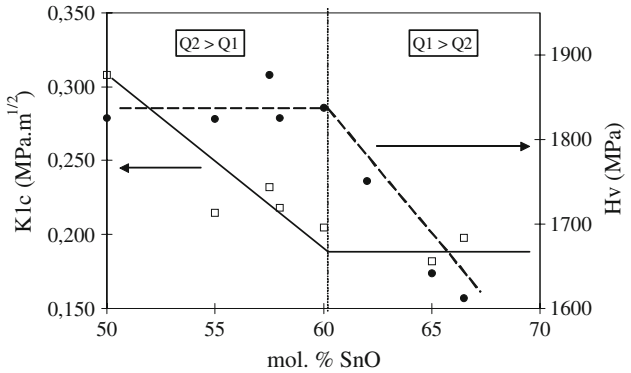

Fig. 8 Vickers microhardness (H_v) and fracture toughness (K_{1c}) as a function of the tin oxide molar content

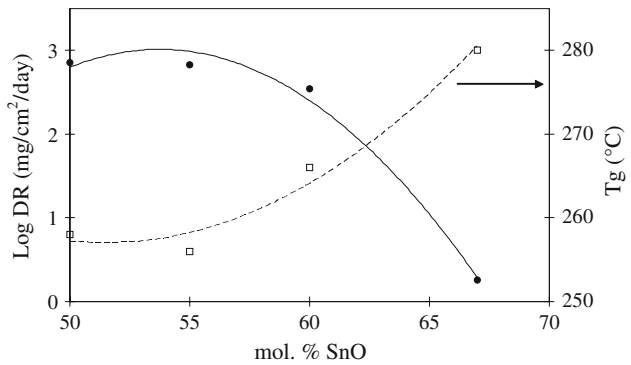

Fig. 9 Dissolution rate (DR) as a function of the tin oxide content (T = 95 °C and (S/V) ratio of 0.1 cm^{-1}). The corresponding values of T_g are given for illustration

is first decreasing and turns out to be constant when the Q^1 units become the most numerous.

Figure 9 shows the dissolution rate of the $Sn(PO_3)_2$ to $Sn_2P_2O_7$ glass compositions performed at the temperature of 95 °C with a constant (S/V) ratio of 0.1 cm^{-1}. It clearly demonstrates the composition dependence of the durability and the existence of a structural effect, which is

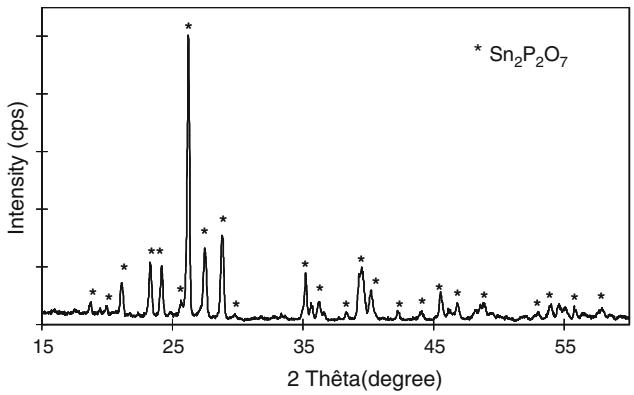

Fig. 10 X-ray diffraction pattern of a $Sn_2P_2O_7$ crystallized sample

also illustrated by the composition dependence of the glass transition temperature. The corrosion of phosphate glasses is assumed to occur by the hydration of P–O–P bonds, which breaks the tetrahedra chains. Whereas the metaphosphate glasses are composed of PO_4 tetrahedra chains with two P–O–P bonds per tetrahedron, the pyrophosphate is composed of Q^1-type sites that means only one P–O–P bond between two PO_4 tetrahedra. It is clear that an increase of the O/P atomic ratio leads to an improvement of the chemical durability, by substituting P–O–P bonds by Sn–O–P bonds. Nevertheless, for compositions with an atomic ratio in the range from 3 to 3.5, the dissolution rate is relatively constant and close to 3 mg cm^{-2} day^{-1}. This value decreases drastically to 0.25 mg cm^{-2} day^{-1} for the pyrophosphate composition (O/P = 3.5). In other terms, the chemical durability is improved more than 300 times following a more general trend [14].

Differential thermal analysis experiments performed on each glass sample have shown that only the pyrophosphate composition exhibits a crystallization exotherm. The X-ray diffraction pattern (see Fig. 10), recorded at room temperature after heating at 450 °C during 1 h, reveals the presence of the low-temperature form of the crystalline pyrophosphate recently identified by Chernaya et al. [15]. No reversible transition to the high temperature phase was evidenced by DTA experiments.

Conclusions

A microwave-heating device has been used to prepare tin phosphate glasses. Melting temperatures up to 950 °C and melting times no longer than 10 min have allowed to limit the oxidation of tin. Thus, the Sn^{4+}/Sn_{total} ratio, determined from Mössbauer experiments, does not exceed 6 at.%. As expected, the glass transition temperature and the density increase with the SnO content. Some of the mechanical characteristics, like the fracture toughness or the Vickers microhardness, are very sensitive to the depolymerization of the vitreous network and some are not, like the elastic moduli or the thermal expansion coefficient. The chemical durability of tin phosphate glasses is low except for the pyrophosphate composition, which is 300 times more durable than the metaphosphate one, confirming the depolymerization dependence of the durability. Concerning the crystallization behaviour, only the pyrophosphate composition is able to devitrify giving the low temperature crystalline phase of $Sn_2P_2O_7$.

References

1. Donald IW (1993) J Mater Sci 28:2841. doi:10.1007/BF00354689
2. Hudecek J (1991) Engineered materials handbook, vol 4. ASM International, Metals Park, p 1069
3. US Federal Registry (1979) 44:60980
4. Morena R (2000) J Non-Cryst Solids 263 & 264:382
5. Holland D, Howes AP, Smith ME, Hannon AC (2002) J Phys Condens Matter 14:13609
6. Vaidhyanathan B, Ganguli M, Rao KJ (1994) J Solid State Chem 113:448
7. Vaidhyanathan B, Prem Kumar C, Rao JL et al (1998) J Phys Chem Solids 59:121
8. Ghussn L, Martinelli JR (2004) J Mater Sci 39:1371. doi: 10.1023/B:JMSC.0000013899.75724.e1
9. Massiot D, Fayon F, Capron M, King I, Le Calvé S, Alonso B, Durand J-O, Bujoli B, Gan Z, Hoatson G (2002) Magn Reson Chem 40:70
10. Blessing GV (1990) Dynamic elastic modulus measurements in materials, ASTM STP 1045. ASTM, Philadelphia
11. Lippma E, Magi M, Samoson A, Engelhardt G, Grimmer A (1980) J Am Chem Soc 102:4889
12. Van Wazer JR (1958) Phosphorus and its compounds. Interscience, New York
13. Bekaert E, Montagne L, Delevoye L, Palavit G, Revel B (2004) CR Chim 7:377
14. Day DE, Wu Z, Ray CS, Hrma P (1998) J Non-Cryst Solids 241:1
15. Chernaya VV, Mitiaev AS, Chizhov PS, Dikarev EV, Shpanchenko RV, Antipov EV, Korolenko MV, Fabritchnyi PB (2005) Chem Mater 17:284